J Mol Model (2013) 19:647–659
DOI 10.1007/s00894-012-1592-z

ORIGINAL PAPER

DFT investigations of phosphotriesters hydrolysis in aqueous solution: a model for DNA single strand scission induced by N-nitrosoureas

Tingting Liu · Lijiao Zhao · Rugang Zhong

Received: 23 February 2012 / Accepted: 23 August 2012 / Published online: 22 September 2012

Abstract DNA phosphotriester adducts are common alkylation products of DNA phosphodiester moiety induced by N-nitrosoureas. The 2-hydroxyethyl phosphotriester was reported to hydrolyze more rapidly than other alkyl phosphotriesters both in neutral and in alkaline conditions, which can cause DNA single strand scission. In this work, DFT calculations have been employed to map out the four lowest activation free-energy profiles for neutral and alkaline hydrolysis of triethyl phosphate (TEP) and diethyl 2-hydroxyethyl phosphate (DEHEP). All the hydrolysis pathways were illuminated to be stepwise involving an acyclic or cyclic phosphorane intermediate for TEP or DEHEP, respectively. The rate-limiting step for all the hydrolysis reactions was found to be the formation of phosphorane intermediate, with the exception of DEHEP hydrolysis in alkaline conditions that the decomposition process turned out to be the rate-limiting step, owing to the extraordinary low formation barrier of cyclic phosphorane intermediate catalyzed by hydroxide. The rate-limiting barriers obtained for the four reactions are all consistent with the available experimental information concerning the corresponding hydrolysis reactions of phosphotriesters. Our calculations performed on the phosphate triesters hydrolysis predict that the lower formation barriers of cyclic phosphorane intermediates compared to its acyclic counter-part should be the dominant factor governing the hydrolysis rate enhancement of DEHEP relative to TEP both in neutral and in alkaline conditions.

Keywords Acyclic phosphorane · Cyclic phosphorane · Diethyl 2-hydroxyethyl phosphate · Hydrolysis mechanism · Triethyl phosphate

Introduction

N-nitrosoureas are an important family of alkylating agents widely used in the clinical treatment of cancer including leukemia, Hodgkin's disease and various solid tumors [1, 2]. This kind of compound was generally accepted to decompose chiefly into a diazohydroxide and an organic isocyanate in physiological condition without metabolism (Scheme 1). Particularly, the diazohydroxide and its decomposed products were considered to be responsible for various DNA lesions including misparing, miscoding, and single strand break by reacting with the nucleophilic sites of DNA. The phosphodiester moiety is one of the major DNA alkylation sites for various N-nitrosoureas, leading to different kinds of DNA phosphotriester adducts (Scheme 1) [3–6]. In the reaction of ethylnitrosoureas (ENUs) with DNA in vitro and in cell suspension, ethyl phosphotriester was found to be the predominant ethylated products with the content of 50–60 % [7–9]. The phosphodiester moiety is also an alkylation site for chloroethylnitrosoureas (CENUs) [6, 10, 11], which results in both 2-chloroethyl phosphotriesters and 2-hydroxyethyl phosphotriesters.

The hydroxyethylations of phosphodiesters in DNA by CENUs or hydroxyethylnitrosoureas (HENUs) have been reported to result in single strand breaks both in neutral and in alkaline conditions [12–17]. Further studies [18–23] of model compounds indicated that the stabilities of phosphotriesters extremely depended on the nature of the alkyl groups transferred to phosphate residual from alkylating species. In previous works [18, 21, 22], a series of phosphate triesters (See Chart 1) bearing various functional

Electronic supplementary material The online version of this article (doi:10.1007/s00894-012-1592-z) contains supplementary material, which is available to authorized users.

T. Liu · L. Zhao (✉) · R. Zhong
College of Life Science and Bioengineering,
Beijing University of Technology,
Beijing 100124, China
e-mail: zhaolijiao@bjut.edu.cn

Scheme 1 DNA phosphotriester adducts induced by N-nitrosoureas

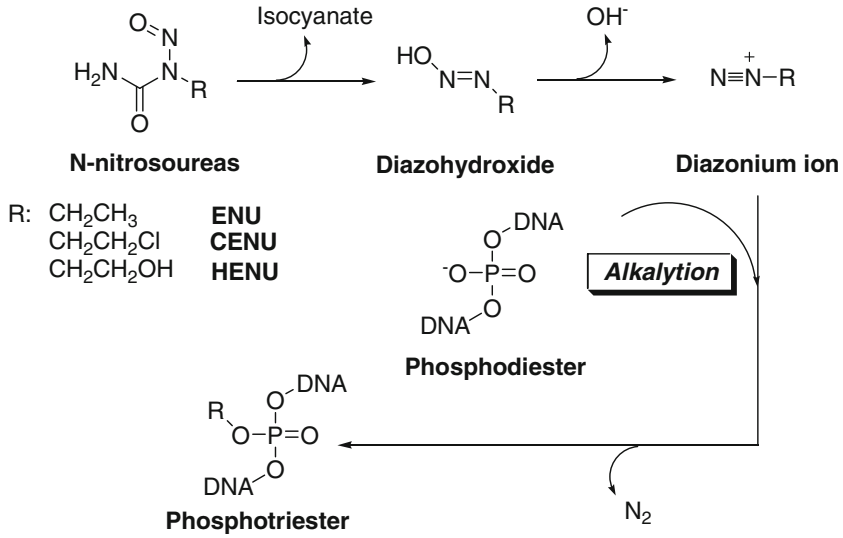

groups in the 2-position of one ethyl moiety, including triethyl phosphate (TEP), diethyl 2-chloroethyl phosphate (DECEP), diethyl 2-methoxyethyl phosphate (DEMEP) and diethyl 2-hydroxyethyl phosphate (DEHEP), were used as model compounds to assess the stabilities of DNA phosphotriester adducts arising from N-nitrosoureas. Their results showed that the hydrolysis of all the alkyl phosphate triesters was base-catalyzed. However, DEHEP has been observed to hydrolyze more rapidly than other alkyl phosphate triesters in aqueous solutions by Conrad et al. [23]: in neutral conditions, all the alkyl phosphate triesters were extremely stable [19, 20, 23], only DEHEP was observed to slowly hydrolyze; in alkaline conditions (pH 12.5), the half-life of alkyl phosphate triesters were several hundred hours except for DEHEP with a half-life of about 1 min. On the basis of these experimental observations, all the alkyl phosphate triesters were supposed to decompose in the same way with the exception of DEHEP, which was presumed to undergo a much lower activation energy hydrolysis pathway depending on the availability of a free 2-hydroxy functional group. Moreover, the biological activities of various hydroxyalkylnitrosourea analogs were compared by Zeller et al. [24, 25] drawing a conclusion that DNA single strand breaks were related to carcinogenicity but not to anticancer effectiveness. Accordingly, thoroughly understanding the mechanism of phosphotriester hydrolysis in solution is crucial for further understanding the relationship between the structures and the biochemical activities of N-nitrosoureas.

In recent years, a number of theoretical studies [26–54] of the hydrolysis mechanisms of phosphate esters have been reported. The majority of them were carried out on the hydrolysis of acyclic phosphate monoesters and diesters, whereas only a few studies [38–42] were performed on the hydrolysis of acyclic phosphate triesters. In particular, the alkaline hydrolysis of trimethyl phosphate (TMP) was fully investigated by Chang et al. using ab initio molecular orbital calculations in gas phase and in solution [39, 40]. In these studies, the hydrolysis reaction pathway of TMP initiated by the nucleophilic addition of a hydroxide anion at phosphorus was revealed as a stepwise pathway involving an acyclic phosphorane triester intermediate (see Chart 2), followed by

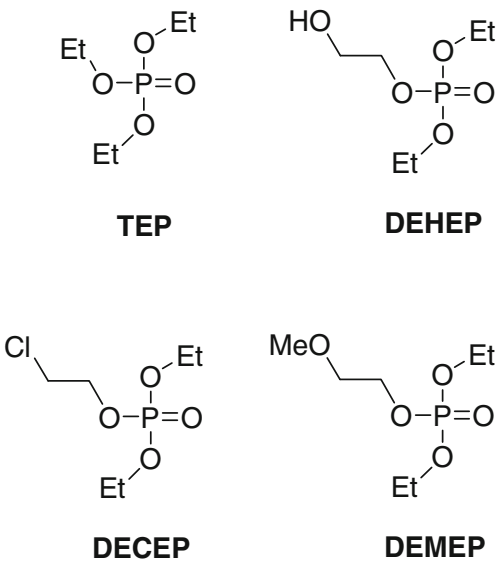

Chart 1 2-Substituent ethyl phosphate triesters

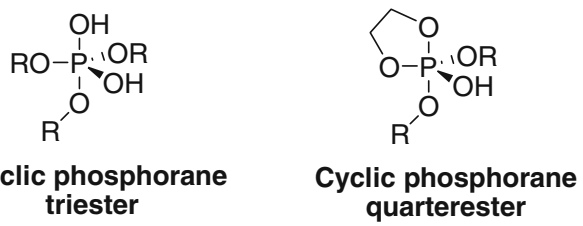

Chart 2 Acyclic and cyclic phosphorane esters

pseudorotation [55] and subsequent cleavage of phosphate ester bond with simultaneous intramolecular proton transfer. Furthermore, the DFT calculations in aqueous solution were employed to study the hydroxide-catalyzed P−O cleavage reactions of TMP by Iche-Tarrat et al. [41]. Lately, they expanded the research to six different dimethylphosphate triesters, revealing that the alkaline hydrolysis of esters with poor leaving groups occurs via a stepwise mechanism, whereas for good leaving groups, it occurs via a concerted mechanism [42]. However, the hydrolysis mechanisms of alkyl phosphate triesters in neutral conditions have never been investigated in theoretical methods (to our knowledge).

In previous studies about the stereochemistry of phosphates by Brown et al. [56, 57], an intramolecular reaction was postulated to be the dominant pathway of the hydrolysis of 2-hydroxyalkyl phosphates, which was initiated by the nucleophilic attack of 2-hydroxyalkyl group at phosphorus resulting in a cyclic phosphorane quaterester intermediate (see Chart 2) containing a five-membered dioxaphospholane ring. A similar mechanism was also proposed [58] for the hydrolysis of RNA with the participation of 2′-OH group of sugar moiety, involving an analogous cyclic phosphorane triester intermediate. The properties of cyclic phosphorane diesters and triesters have been investigated in the calculations [40, 43–53] on the hydrolysis of corresponding cyclic ethylene phosphate (EP) and methyl ethylene phosphate (MEP) [59]. Unfortunately, the properties of cyclic phosphorane quateresters have not been fully understood.

In this work, TEP and DEHEP were employed as the model compounds to investigate the mechanistic details of the hydrolysis of DNA phosphate adducts induced by N-nitrosoureas by quantum mechanical calculations in aqueous solution. Calculations were preformed using density functional theory (B3LYP function) at the basis set levels of 6–311++G(3df,2p)/6–31++G(d,p). Solvation was approximated by the conductor-like polarizable continuum model (CPCM) [60–62]. For TEP, the reactions initiated by water or hydroxide attack at phosphorus atom were constructed to simulate the hydrolysis under neutral or alkaline conditions, respectively. For DEHEP, the intermolecular reactions initiated by 2-hydroxyethyl group attack at phosphorus atom were considered as the main hydrolysis route. For this system, a water molecule or a hydroxide anion was also included in the nucleophilic addition process to discriminate the hydrolysis in neutral or in alkaline conditions. Four free energy profiles for the hydrolysis of TEP and DEHEP in both neutral and alkaline conditions were mapped out to confirm the lowest activation free energy pathways and the rate-limiting steps. Furthermore, the activation free energies of each step in these reaction pathways were compared to interpret the distinct hydrolysis rates of TEP and DEHEP. This research provides theoretical evidence for the hypothesis that a base-catalyzed formation of the cyclic phosphorane quaterester intermediate is the key process for the rapid hydrolysis of 2-hydoxyalkyl phosphate DNA adducts, and further serves as an elicitation for more active and less toxic anticancer drugs containing N-nitrosourea moiety.

Theoretical calculations

All the structures were optimized with the Kohn-Sham density functional theory (DFT) methods, using the hybrid exchange functional of Becke [63] and correlation functional of Lee, Yang, and Parr [64] (B3LYP) with a 6–31++G(d,p) basis set. Because all processes of DNA damages involved in the anticancer or carcinogenic process are supposed to take place in aqueous solution, the solvent effect of water on all reactions was taken into account. The geometric structures of all reactants, transition states, intermediates and products were fully optimized by employing self-consistent reaction field (SCRF) computations using the conductor-like polarizable continuum model (CPCM) [65, 66] without imposed constraints. By default, the molecular cavity was built up using the UFF radii, which places a sphere around reach solute atom, with the radii scaled by a factor of 1.1. Frequency calculations were performed at the same theoretical level to verify the nature of the stationary points on the potential energy surface (PES); i.e., that there were no imaginary frequencies for minima and only one imaginary frequency for transition states. Furthermore, the intrinsic reaction coordinate (IRC) calculations were performed to confirm that every transition state connects the corresponding reactant and product through the minimized-energy pathway.

For obtaining the energetic data with higher accuracy, the single-point energy of each stationary point was refined by using a larger 6–311++G(3df,2p) basis set, on the basis of optimized geometries at the B3LYP/6–31++G(d,p)/CPCM level, also denoted as B3LYP/6–311++G(3df,2p)/CPCM//B3LYP/6–31++G(d,p)/CPCM. The single-point energy calculation with B3LYP has been found to be in reasonably good agreement with the one obtained from CCSD(T) [67, 68], therefore this density functional protocol has been extensively applied in previous investigations for biological phosphate system [49, 50, 54, 69, 70]. The zero-point energy (ZPE), thermal contributions to the enthalpy (ΔH), entropy (ΔS), and Gibbs free energy (ΔG) at T=298 K within the harmonic oscillator approximation in the canonical ensemble [54, 55] were evaluated by frequency calculations at the B3LYP/6–31++G(d,p)/CPCM theoretical level. Recent theoretical studies [41, 52] have reported that the rigid rotor-harmonic oscillator approximation [71] may induce an overestimation of the entropic contribution to the absolute values of the activation free energies in phosphate hydrolysis. However, it was considered [59] to scarcely affect the

relative energetic values of the species involved in this work. All computations presented here were performed with GAUSSIAN 09 program package [72].

Results and discussion

Neutral hydrolysis of TEP

All the possible reaction pathways of TEP in neutral hydrolysis initiated by water attack at phosphorus are depicted in Scheme 2. The corresponding free energy profile is shown in Fig. 1 and all the thermodynamic data are listed in Table 1. The solution structures of transition states and intermediates involved in the processes are given in Fig. 2 and all the remaining optimized geometries are shown in Fig. S1 in the Supporting information. The selected structural parameters are listed in Table S1 and S5.

The first step of this reaction is the nucleophilic addition of water at phosphorus atom through an associative transition state (**TS1**) with the forming bond P−O5 distance of 2.17 Å, resulting in the formation of a neutral acyclic phosphorane intermediate (**Int1**). This intermediate has a trigonal bipyramidal (TBP) geometry with the P−O1, P−O2, and P−O3 group equatorial and the P−O4 and P−O5 group axial. As shown in Scheme 2 and Fig. 1, **Int1** can transform to the isomers **Int2** and **Int3** though two different reaction pathways. Firstly, the equatorial O1−H1 group aligned with the P−O5 bond in **Int1** turns around to be aligned with the P−O4 bond resulting in an analogous intermediate (**Int2**) via a transition state (**TS2**) with the free-energy barrier of 8.1 kcalmol^{-1}. Alternatively, **Int1** can undergo pseudorotation via **TS3**, yielding a stereoisomer (**Int3**) with the P−O1, P−O4, and P−O5 group equatorial and the P−O2 and P−O3 group axial. The activation free energy of pseudorotation is 6.6 kcalmol^{-1}, which is slightly lower than the value (8.1 kcalmol^{-1}) of hydroxyl group rotation.

According to the structure parameters listed in Table S1, the orientation of equatorial hydroxyl group was found to have a significant influence on the distance of the axial P−

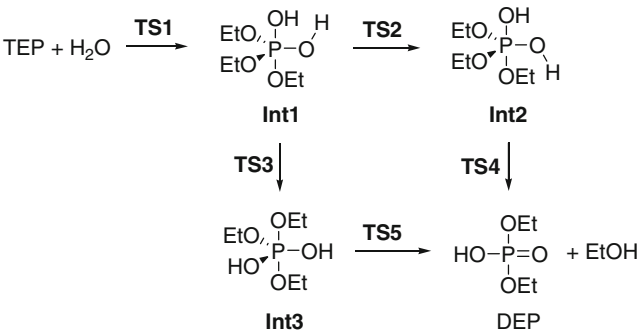

Scheme 2 Neutral hydrolysis pathways of TEP

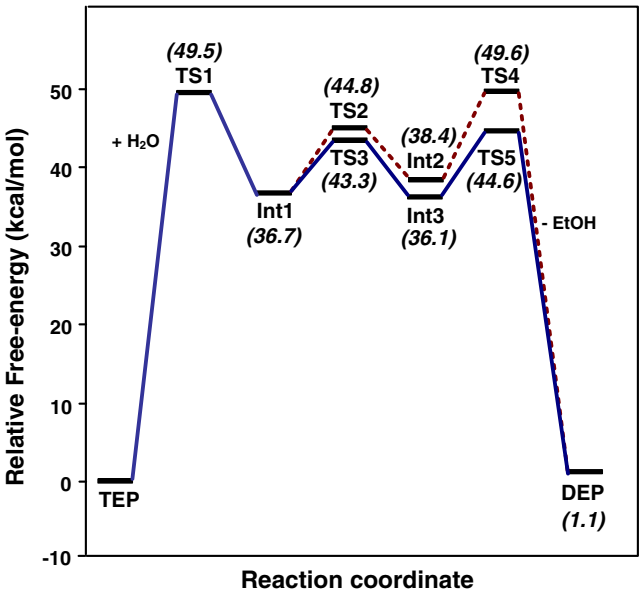

Fig. 1 Free-energy profile (kcalmol^{-1}) for the neutral hydrolysis of TEP obtained at B3LYP/6–311++G(3df,2p)/CPCM//B3LYP/6–31++G(d,p)/CPCM theoretical level

O_{Et} bond in phosphorane intermediates, as noted in the earlier works [38, 41, 53, 54]. In **Int2**, the equatorial O1−H1 group was rotated to be aligned with P−O4 bond, which lengthens the distance of axial P−O4 bond from 1.68 Å in **Int1** to 1.70 Å. In **Int3**, there are two hydroxyl groups O1−H1 and O5−H5 situated at the equatorial positions through the pseudorotation, and the orientations of them were both aligned with the axial P−O3 bond. Accordingly, the distance of P−O3 bond in **Int3** was lengthened to 1.73 Å, which is obviously longer than the distance (1.70 Å) of P−O4 bond in **Int2**.

The conformations of **Int2** and **Int3** (Fig. 2) are both associated with an intramolecular hydrogen bond O_{eq}···H···O_{axi}

Table 1 Activation energies (ΔE), enthalpies (ΔH), entropies (ΔS) and free energies (ΔG) for the neutral hydrolysis of TEP calculated at B3LYP/6–311++G (3df,2p)//B3LYP/6–31++G(d,p) level in the solution phase

Species	ΔE	ΔH	ΔS	ΔG
TEP+H_2O	0.0	0.0	0.0	0.0
TS1	38.0	36.7	−42.9	49.5
Int1	22.0	23.6	−43.9	36.7
TS2	30.6	31.2	−45.6	44.8
Int2	23.6	25.2	−44.3	38.4
TS3	28.2	29.0	−48.0	43.3
Int3	20.8	22.6	−45.3	36.1
TS4	39.1	37.5	−40.6	49.6
TS5	32.9	32.4	−40.9	44.6
DEP+EtOH	1.3	1.5	1.3	1.1

Units are kcalmol^{-1} for energies and calmol^{-1} deg^{-1} for entropies

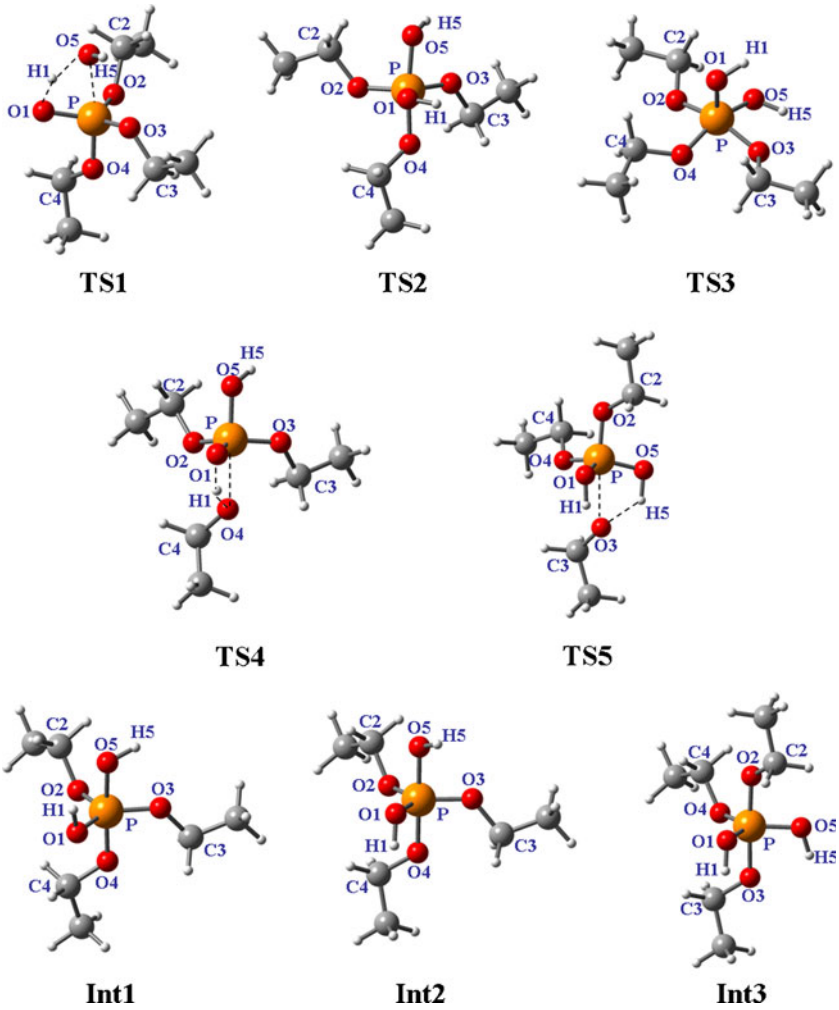

Fig. 2 Solution phase optimized structures of the transition states and the intermediates involved in the neutral hydrolysis of TEP

between the equatorial hydroxyl group and the oxygen on the axial P−O_{Et} group. Consequently, the two acyclic phosphoranes can both decompose by concerted reactions via **TS4** or **TS5** with the proton on hydroxyl group transferring onto the leaving group, resulting in an ethanol (EtOH) and a neutral diethyl phosphate (DEP). Furthermore, the activation free energy of **TS5** (8.5 kcalmol^{-1}) is remarkably lower than the value of **TS4** (11.2 kcalmol^{-1}), which can be attributed to the spatial structure of the equatorial hydroxyl group in the acyclic phosphorane intermediates mentioned above,.

The free energy profile for this system (Fig. 1) indicates that the lowest energy pathway is nucleophilic addition of water molecule at phosphorus via **TS1**, followed by pseudorotation of **Int1** via **TS3** resulting in **Int3**, and subsequent elimination via **TS5** with simultaneous intramolecular proton transfer to yield EtOH and DEP. Obviously, the rate-limiting step of the reaction pathway is the water nucleophilic addition process (the formation of neutral acyclic phosphorane), which has a free energy barrier of 49.5 kcal mol^{-1}. Accordingly, we can conclude that the extreme stability of TEP in neutral solutions observed in the previous works [19, 20, 23] can be attributed to the large activation energy of neutral acyclic phosphorane formation.

Alkaline hydrolysis of TEP

All the possible reaction pathways of TEP in alkaline hydrolysis initiated by hydroxide attack at phosphorus are depicted in Scheme 3. The corresponding free energy profile

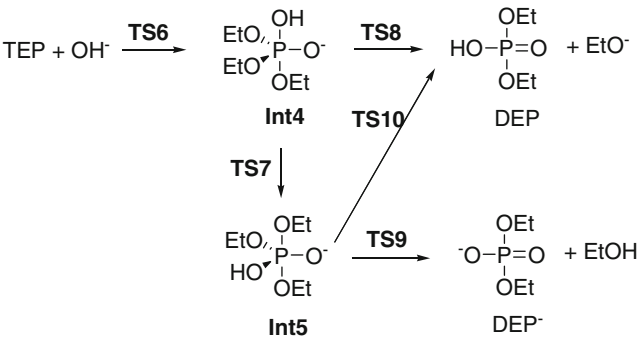

Scheme 3 Alkaline hydrolysis pathways of TEP

is shown in Fig. 3 and all the thermodynamic data are listed in Table 2. The solution structures of transition states and intermediates involved in the processes are given in Fig. 4 and all the remaining optimized geometries are shown in Fig. S1 in the Supporting information. The selected structural parameters are listed in Table S2 and S5.

Unlike water attack reactions, the nucleophilic addition of hydroxide at phosphorus atom proceeds via a transition state (**TS6**) without proton migration between nucleophile and substrate. **TS6** is formed at a P−O5 distance of 2.48 Å, leading to a monoanionic acyclic phosphorane intermediate (**Int4**). The free-energy barrier of this step is 25.7 kcalmol^{-1}, which is about 23.8 kcalmol^{-1} lower than the barrier of water addition step. This result indicates that the formation of phosphorane intermediate can be catalyzed by hydroxide. The bond angle O5−P−O4 in monoanionic **Int4** is more distorted compared with the neutral specie **Int1** (162.3° in **Int4** vs 174.3° in **Int1**), which facilitate the pseudorotation with a much lower energy barrier of 1.5 kcalmol^{-1} (**TS7**) compared to in neutral conditions (6.6 kcalmol^{-1}). Therefore, we can interpret that the pseudorotation of monoanionic acyclic phosphorane can proceed faster than the neutral ones. Alternatively, **Int4** can undergo a direct cleavage of the axial P−O4 bond without proton migration yielding an ethoxide (EtO^-) and a DEP via a transition state (**TS8**) with an activation free energy of 9.4 kcalmol^{-1}.

In pseudorotation, the hydroxyl group (O5−H5) at the axial position in **Int4** rotates around to the equatorial position resulting in a lower energy stereoisomer (**Int5**). In this isomer (**Int5**), the axial bond length of P−O2 and P−O3 are

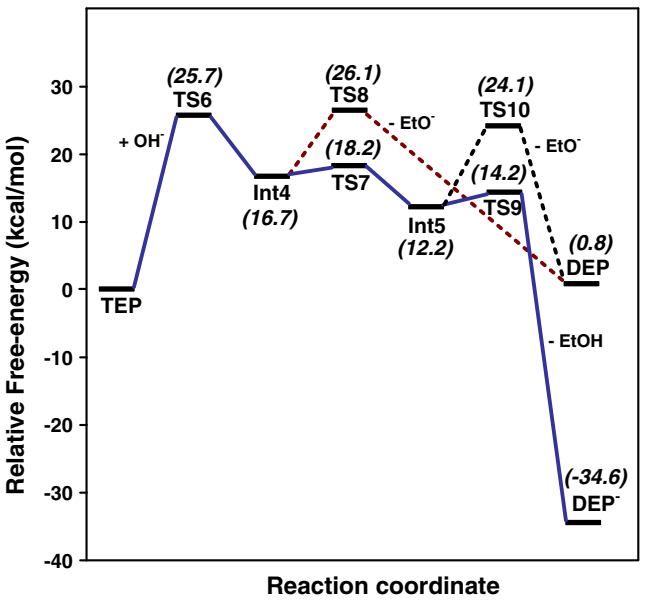

Fig. 3 Free-energy profile (kcalmol^{-1}) for the alkaline hydrolysis of TEP obtained at B3LYP/6–311++G(3df,2p)/CPCM//B3LYP/6–31++G (d,p)/CPCM theoretical level

Table 2 Activation energies (ΔE), enthalpies (ΔH), entropies (ΔS) and free energies (ΔG) for the alkaline hydrolysis of TEP calculated at B3LYP/6–311++G (3df,2p)//B3LYP/6–31++G(d,p) level in the solution phase

Species	ΔE	ΔH	ΔS	ΔG
TEP+OH^-	0.0	0.0	0.0	0.0
TS6	14.2	14.5	−37.6	25.7
expt[a]	——	14.1	−34.2	24.3
Int4	3.4	4.6	−40.6	16.7
TS7	3.8	4.4	−46.3	18.2
Int5	−1.4	−0.1	−41.3	12.2
TS8	15.3	15.1	−36.9	26.1
TS9	3.5	3.4	−36.2	14.2
TS10	12.6	12.4	−39.2	24.1
DEP+EtO^-	2.9	2.0	4.0	0.8
DEP^-+EtOH	−34.3	−33.7	3.0	−34.6

Units are kcalmol^{-1} for energies and calmol^{-1} deg^{-1} for entropies

[a] Experimental enthalpy and free energy of activation taken from reference 71

1.75 and 1.80 Å, respectively. The cleavage of them can result in two different sets of hydrolysis products. Firstly, the cleavage of the axial P−O3 bond that is cis to the equatorial O5−H5 group can result in the products composed of EtOH and DEP^- via **TS9** with simultaneous proton transfer, which is in accordance with the process in neutral conditions (**TS4** and **TS5**). Alternatively, **Int5** can also yield the product composed of EtO^- and DEP via the direct cleavage of the axial P−O2 bond that is trans to the equatorial O5−H5 group via **TS10** as the cleavage of the P−O4 bond in **Int4** via **TS8**. The activation free energy of the cleavage of P−O3 bond with proton transfer (**TS10**) is only 2.0 kcalmol^{-1}, which is much lower than the barrier (11.9 kcalmol^{-1}) of the direct cleavage (**TS9**) of P−O2 bond without proton transfer. Clearly, the cleavage of axial P−O_{Et} bond in monoanionic phosphorane intermediate is extremely promoted by the proton of equatorial hydroxyl group.

The free energy profile for the alkaline hydrolysis of TEP (Fig. 3) indicates that the lowest free energy pathway is the nucleophilic addition of hydroxide via **TS6**, followed by pseudorotation of **Int4** via **TS7** leading to **Int5**, and subsequent elimination via **TS9** with simultaneous intramolecular proton transfer to yield EtOH and DEP^-. This result is in agreement with the previous calculations about the alkaline hydrolysis of TMP [39, 41]. The rate-limiting step of this reaction pathway is also the nucleophilic addition step as the neutral hydrolysis of TEP. Furthermore, the activation free energies of formation and decomposition of the monoanionic acyclic phosphorane intermediate are both apparently lower than the values of neutral one, especially for the formation step, which is about 23.8 kcalmol^{-1} lower than the value in neutral hydrolysis. This result suggests that the

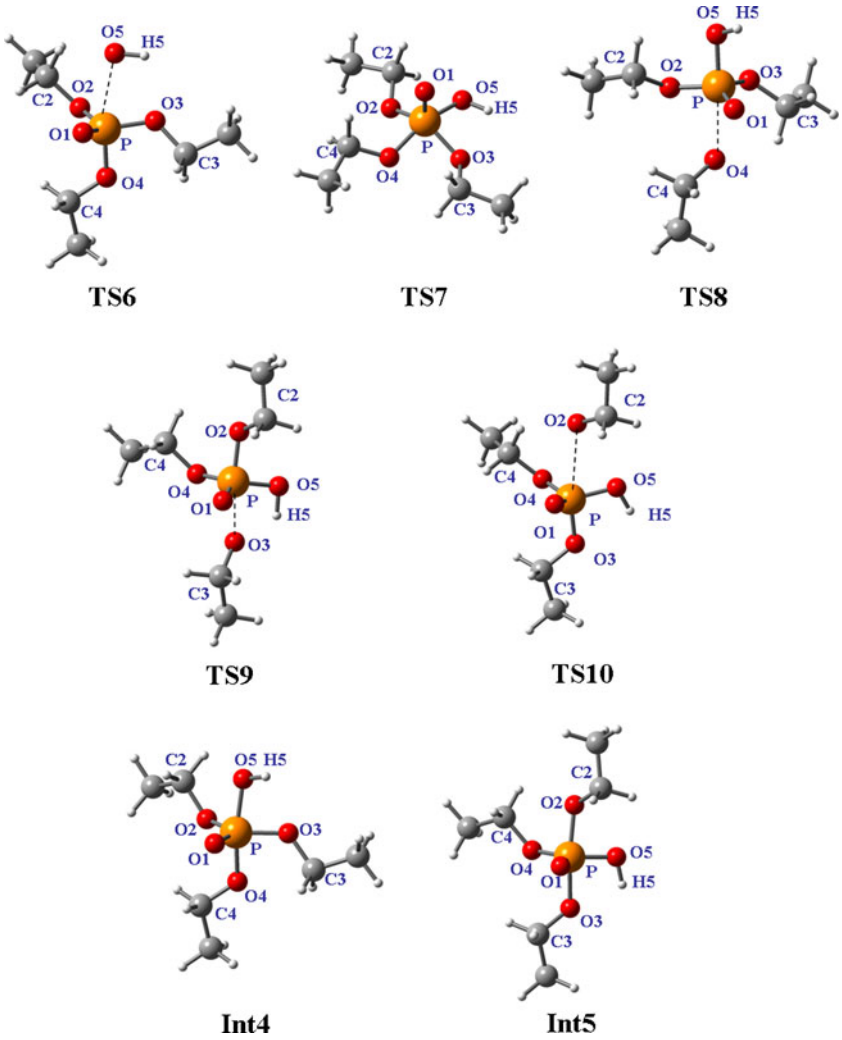

Fig. 4 Solution phase optimized structures of the transition states and the intermediates involved in the alkaline hydrolysis of TEP

hydrolysis of TEP can be catalyzed by hydroxide, which is consistent with the observations that TEP is more likely to undergo hydrolysis in alkaline conditions than in neutral conditions [18, 21, 22].

The thermodynamic data summarized in Table 2 illuminate that the calculated activation enthalpy (14.5 kcalmol^{-1}) for TEP hydrolysis in alkaline conditions is in excellent agreement with the experimentally determined value [73] (14.1 kcalmol^{-1}) at 25 °C. More negligible errors were made in the calculation of the activation entropy compared to the multipolar expansion (MPE) B3LYP calculations on the alkaline hydrolysis of TMP [41]. The discrepancy between the calculated value (−37.6 calmol^{-1}deg^{-1}) and the experimental one (−34.2 calmol^{-1}deg^{-1}) is only 3.4 calmol^{-1}deg^{-1}. Accordingly, the calculated free energy (25.7 kcalmol^{-1}) is also close to the experimentally derived value (24.3 kcalmol^{-1}).

Neutral hydrolysis of DEHEP

All the possible reaction pathways of DEHEP in neutral hydrolysis initiated by the nucleophilic attack of 2-hydroxyethyl group at phosphorus are depicted in Scheme 4. The corresponding free energy profile is illustrated in Fig. 5 and all the thermodynamic data are listed in Table 3. The solution structures of transition states and intermediates involved in the processes are given in Fig. 6 and all the remaining optimized geometries are shown in Fig. S1 in the Supporting information. The corresponding selected structural parameters are listed in Table S3, S5 and S6.

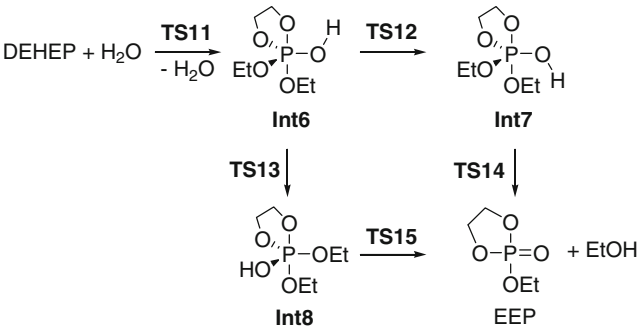

Scheme 4 Neutral hydrolysis pathways of DEHEP

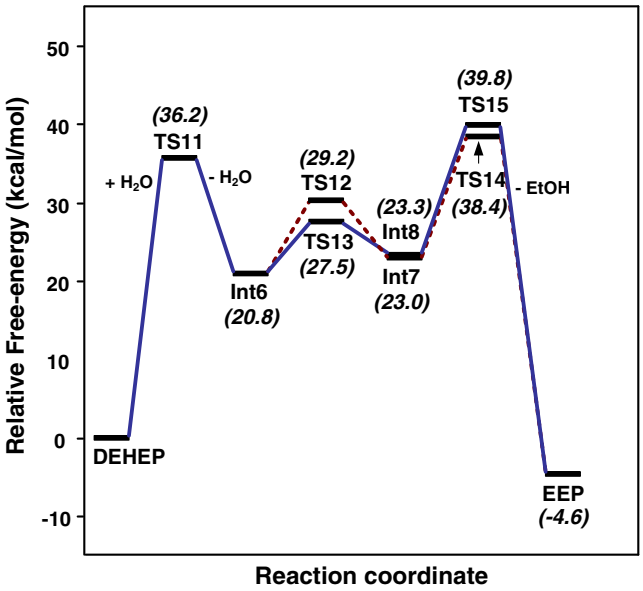

Fig. 5 Free-energy profile (kcal mol^{-1}) for the neutral hydrolysis of DEHEP obtained at B3LYP/6–311++G(3df,2p)/CPCM//B3LYP/6–31++G(d,p)/CPCM theoretical level

As shown in the optimized geometry of **TS11**, the formation of dioxaphospholane ring in neutral conditions is a concerted process of water-mediated hydrogen shift from 2-hydroxyethyl group to phosphoryl group and nucleophilic attack of hydroxyl oxygen on phosphorus. As the P−O5 distance decreases further, a neutral cyclic phosphorane intermediate (**Int6**) with TBP configuration was found with a dioxaphospholane ring formed by P−O2−C2−C5−O5 with dihedral angle O5−C5−C2−O2 of −34.5°, and the hydroxyl group (O1−H6) aligned with the apical endocyclic P−O5 bond.

Subsequently, a couple of stereoisomers (**Int7** and **Int8**) with similar energy values are generated from **Int6** through two different pathways involving the rotation of hydroxyl group (O1−H6) via **TS12** or a pseudorotation process via **TS13**, respectively. It is worth noting that the activation free energy (Fig. 5) of the pseudorotation of the cyclic **Int6** (6.7 kcal mol^{-1}) is very close to the pseudorotation of the acyclic **Int1** (6.6 kcal mol^{-1}) in water attack reactions on TEP, which indicates that the pseudorotation of phosphorane seems to be scarcely affected by the ring strain of pentagon. In addition, the reaction of O1−H6 group rotation has a larger activation free energy of 8.4 kcal mol^{-1} compared with the pseudorotation, similar to the status of **Int1** in the neutral hydrolysis of TEP. Both cyclic isomers (**Int7** and **Int8**) display the conformation that O1−H6 group aligned with the apical exocyclic P−O_{Et} bond, which facilitates an EtOH expulses from the isomers resulting in a cyclic ethyl ethylene phosphate (EEP). The activation free energies of bond cleavage of both isomers via **TS14** and **TS15** are very close, with 15.4 and 16.5 kcal mol^{-1}, respectively. The cyclic EEP and its analogue MEP were reported to hydrolyze rapidly to the acyclic hydroxyethyl phosphate diester with ring opening reaction [74–77].

Table 3 Activation energies (Δ*E*), enthalpies (Δ*H*), entropies (Δ*S*) and free energies (Δ*G*) for the neutral hydrolysis of DEHEP calculated at B3LYP/6–311++G (3df,2p)//B3LYP/6–31++G(d,p) level in the solution phase

Species	Δ*E*	Δ*H*	Δ*S*	Δ*G*
DEHEP+H_2O	0.0	0.0	0.0	0.0
TS11	24.1	20.8	−51.7	36.2
Int6	16.2	16.1	−15.8	20.8
TS12	25.6	24.3	−16.4	29.2
Int7	18.2	18.1	−16.4	23.0
TS13	23.3	22.1	−18.1	27.5
Int8	18.5	18.4	−16.4	23.3
TS14	37.1	33.9	−15.1	38.4
TS15	38.3	35.2	−15.4	39.8
EEP+EtOH	5.7	4.3	29.9	−4.6

Units are kcal mol^{-1} for energies and cal mol^{-1} deg^{-1} for entropies

The free energy profile in Fig. 5 interprets that the most favorable pathway of neutral hydrolysis of DEHEP is the nucleophilic attack of 2-hydroxyethyl group via **TS11**, followed by pseudorotation of **Int6** via **TS13** generating **Int8**, and subsequent elimination via **TS15** with simultaneous intramolecular proton transfer to yield EtOH and EEP. As for the neutral and alkaline hydrolysis of TEP, the rate-limiting step of the neutral hydrolysis of DEHEP is still the nucleophilic attack step. Furthermore, we can see that the formation free energy barrier of neutral cyclic phosphorane (**TS11**) is 36.2 kcal mol^{-1}, which is about 13 kcal mol^{-1} lower than the value of neutral acyclic one (**TS1**); whereas the decomposition free energy barrier of neutral cyclic phosphorane (15.4 kcal mol^{-1}) is obviously larger than the value of neutral acyclic one (8.5 kcal mol^{-1}). So the experimental observation [23] that DEHEP hydrolyzed more rapidly than TEP in neutral conditions can be attributed to the lower formation barrier of neutral cyclic phosphorane than neutral acyclic one, but not to the decomposition of phosphoranes. This result is consistent with the studies of monoanionic methyl 2-hydroxyethyl phosphate diesters (MHEP) hydrolysis by Lim et al. which indicated that the formation activation free energy of the cyclic phosphorane triester in gas phase [45] and in solution [40] were 35.4 and 32.8 kcal mol^{-1}, respectively, and the decomposition activation free energy of cyclic triesters are 9.9 and 10.1 kcal mol^{-1}, respectively. Moreover, Liu et al. [49] also found that the activation free energies of cyclic phosphorane triester formation was much higher than that of the decomposition step.

Alkaline hydrolysis of DEHEP

All the possible reaction pathways of DEHEP in alkaline hydrolysis initiated by the nucleophilic attack of 2-

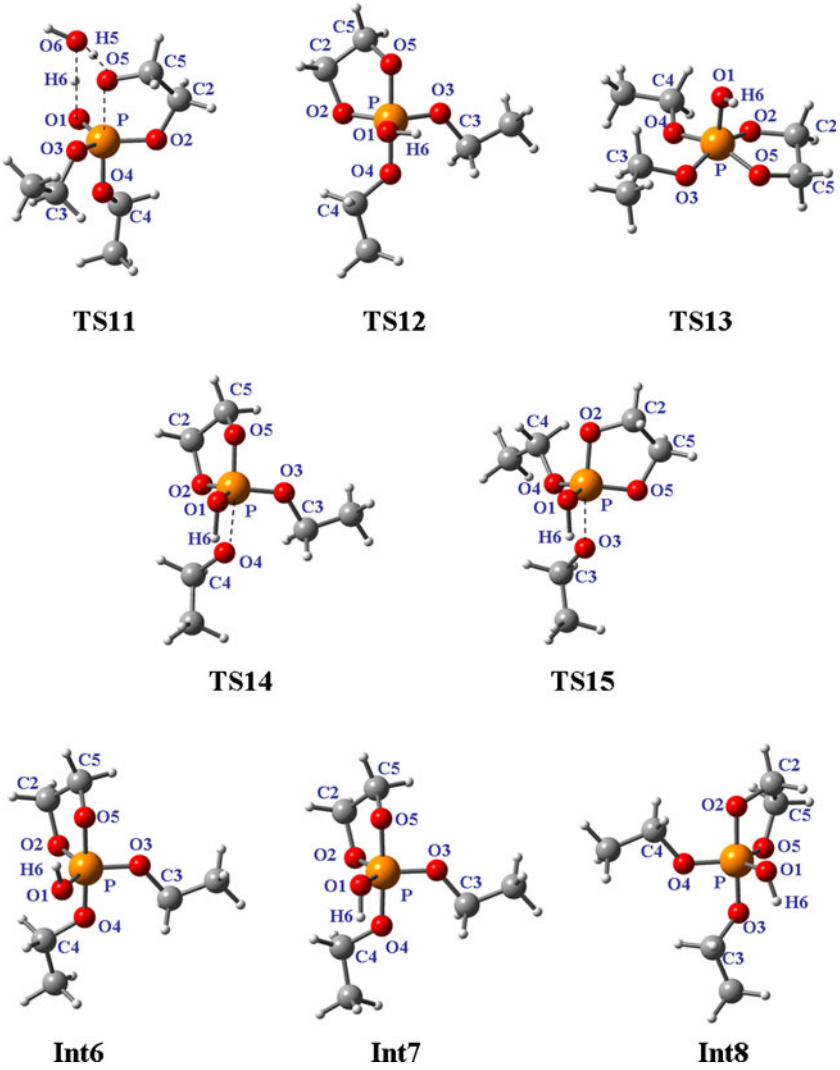

Fig. 6 Solution phase optimized structures of the transition states and the intermediates involved in the neutral hydrolysis of DEHEP

hydroxyethyl group at phosphorus are depicted in Scheme 5. The corresponding free energy profile is illustrated in Fig. 7 and all the thermodynamic data are listed in Table 4. The solution structures of transition states and intermediates involved in the processes are given in Fig. 8 and all the remaining optimized geometries are shown in Fig. S1 in the Supporting information. The selected structural parameters are listed in Table S4, S5 and S6.

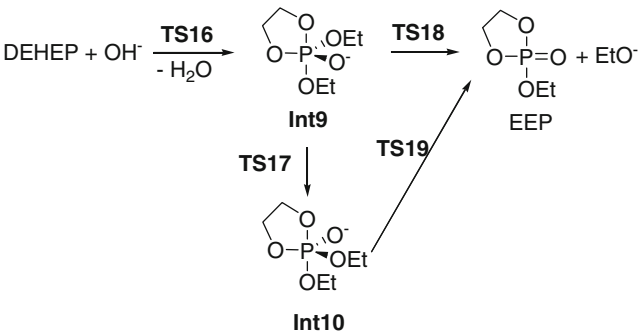

Scheme 5 Alkaline hydrolysis pathways of DEHEP

As shown in the optimized geometry of **TS16**, the atom distances of O5−H5, O6−H5, and P−O5 are 1.56, 1.02 and 2.40 Å, respectively, which indicates that the H5 atom on 2-hydroxyethyl group has already been captured by hydroxide before the P−O5 bond formation. As the atom distance of P−O5 decreases further, a monoanionic cyclic phosphorane intermediate (**Int9**) finally generated with a water molecule. The activation free energy of this step is only 5.3 kcal mol^{-1}, which dramatically decreases about 30.9 kcal mol^{-1} from the value (36.2 kcal mol^{-1}) of **TS11** in the neutral hydrolysis of DEHEP. This result indicates that the formation of cyclic phosphorane quaterester is strongly catalyzed by hydroxide.

As the neutral hydrolysis of DEHEP, the monoanionic **Int9** can also undergo two decomposition pathways as shown in Scheme 5. Owing to the absence of equatorial hydroxyl group in **Int9**, the exocyclic P−O4 bond can cleave directly via **TS18** without proton migration yielding the products composed of EEP and EtO^{-}. The activation free energy of this step is 13.8 kcal mol^{-1}. In the other pathway, **Int9** can transform into its stereoisomer **Int10**

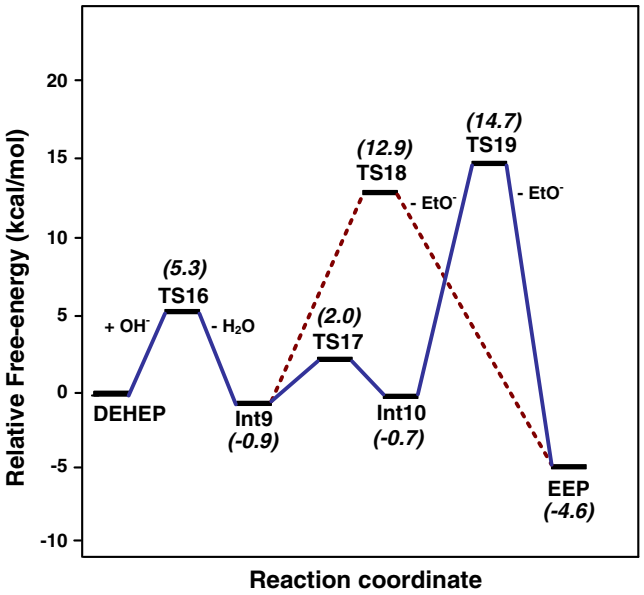

Fig. 7 Free-energy profile (kcal mol^{-1}) for the alkaline hydrolysis of DEHEP obtained at B3LYP/6–311++G(3df,2p)/CPCM//B3LYP/6–31++G(d,p)/CPCM theoretical level

through pseudorotation via **TS17** with a negligible barrier of 2.9 kcal mol^{-1}. Subsequently, **Int10** can lead to the same products as **Int9** through the direct cleavage of the exocyclic P−O3 bond via **TS19** with a free energy barrier of 15.4 kcal mol^{-1}. Compared with the energy barrier of exocyclic P−O_{Et} bond cleavage, the activation free energy of pseudorotation is much lower, so the isomers **Int9** and **Int10** are possible to transform freely through pseudorotation to get the dynamic equilibrium before the cleavage of exocyclic phosphorus ester bond. Accordingly, the monoanionic cyclic phosphorane intermediate may decompose through the pathway with or without pseudorotation equally.

Owing to the activation free energy of nucleophilic attack tremendously declining to 5.3 kcal mol^{-1} in alkaline conditions,

Table 4 Activation energies (ΔE), enthalpies (ΔH), entropies (ΔS) and free energies (ΔG) for the alkaline hydrolysis of DEHEP calculated at B3LYP/6–311++G (3df,2p)//B3LYP/6–31++G(d,p) level in the solution phase

Species	ΔE	ΔH	ΔS	ΔG
DEHEP+OH^-	0.0	0.0	0.0	0.0
TS16	−6.7	−7.0	−41.2	5.3
Int9	−4.1	−4.7	−12.7	−0.9
TS17	−2.2	−3.3	−17.9	2.0
Int10	−3.9	−4.5	−12.6	−0.7
TS18	12.5	10.5	−8.1	12.9
TS19	13.7	11.8	−9.9	14.7
EEP+EtO^-	7.3	4.8	31.6	−4.6

Units are kcal mol^{-1} for energies and cal mol^{-1} deg^{-1} for entropies

the cleavage process of the exocyclic P−O_{Et} bond turns out to be the rate-limiting step with the barrier of 13.8/15.4 kcal mol^{-1}. The similar rate-limiting cleavage of the exocyclic P−O_{Et} bond was also found in the experimental studies of RNA hydrolysis [78–83]. Furthermore, the formation barrier of monoanionic cyclic phosphorane is about 20.4 kcal mol^{-1} lower than the value of monoanionic acyclic phosphorane. This result illuminates that the extremely rapid hydrolysis of DEHEP in alkaline conditions can be attributed to its unusual low formation barrier of dioxaphospholane ring catalyzed by hydroxide.

Conclusions

In this work, in order to clarify the influence of 2-hydroxyethyl group on the decomposition of phosphotriesters, two distinct hydrolysis mechanisms were compared in both neutral and alkaline conditions. Four free energy profiles of all the possible reaction pathways were plotted at B3LYP/6–311++G(3df,2p)/CPCM//B3LYP/6–31++G(d,p)/CPCM theoretical level, and the most energetic favorable pathways were mapped out. Furthermore, the calculated activation free energies of the rate-limiting step in the four reaction pathways were used to illuminate the previous experimental observation that DEHEP hydrolyzed more rapidly than TEP both in neutral and alkaline conditions. All the results and conclusions derived from this work have been summarized as the three main points addressed below.

(1) For TEP, the rate-limiting steps of hydrolysis in neutral and alkaline conditions are both the nucleophile (water or hydroxide) attack at the phosphorus atom, i.e., the formation of acyclic phosphorane. For DEHEP, in neutral conditions, the rate-limiting step is the nucleophilic attack of 2-hydroxyethyl group at phosphorus atom, i.e., the formation of cyclic phosphorane. However, in alkaline conditions, the cleavage of exocyclic P−O_{Et} bond turns into the rate-limiting step instead, i.e., the decomposition of cyclic phosphorane.

(2) In neutral hydrolysis of TEP and DEHEP, the lowest free-energy pathways both are nucleophilic addition at phosphorus, followed by pseudorotation and subsequently decomposition of acyclic or cyclic phosphorane intermediates. In the alkaline hydrolysis, for TEP, the lowest free-energy pathway involves the pseudorotation followed by the decomposition of acyclic phosphorane intermediates; whereas the decomposition of DEHEP can go through either with or without pseudorotation process.

(3) In both neutral and alkaline conditions, the free energy barriers (36.7 and 5.3 kcal mol^{-1}) of the cyclic phosphoranes formation from DEHEP are clearly lower

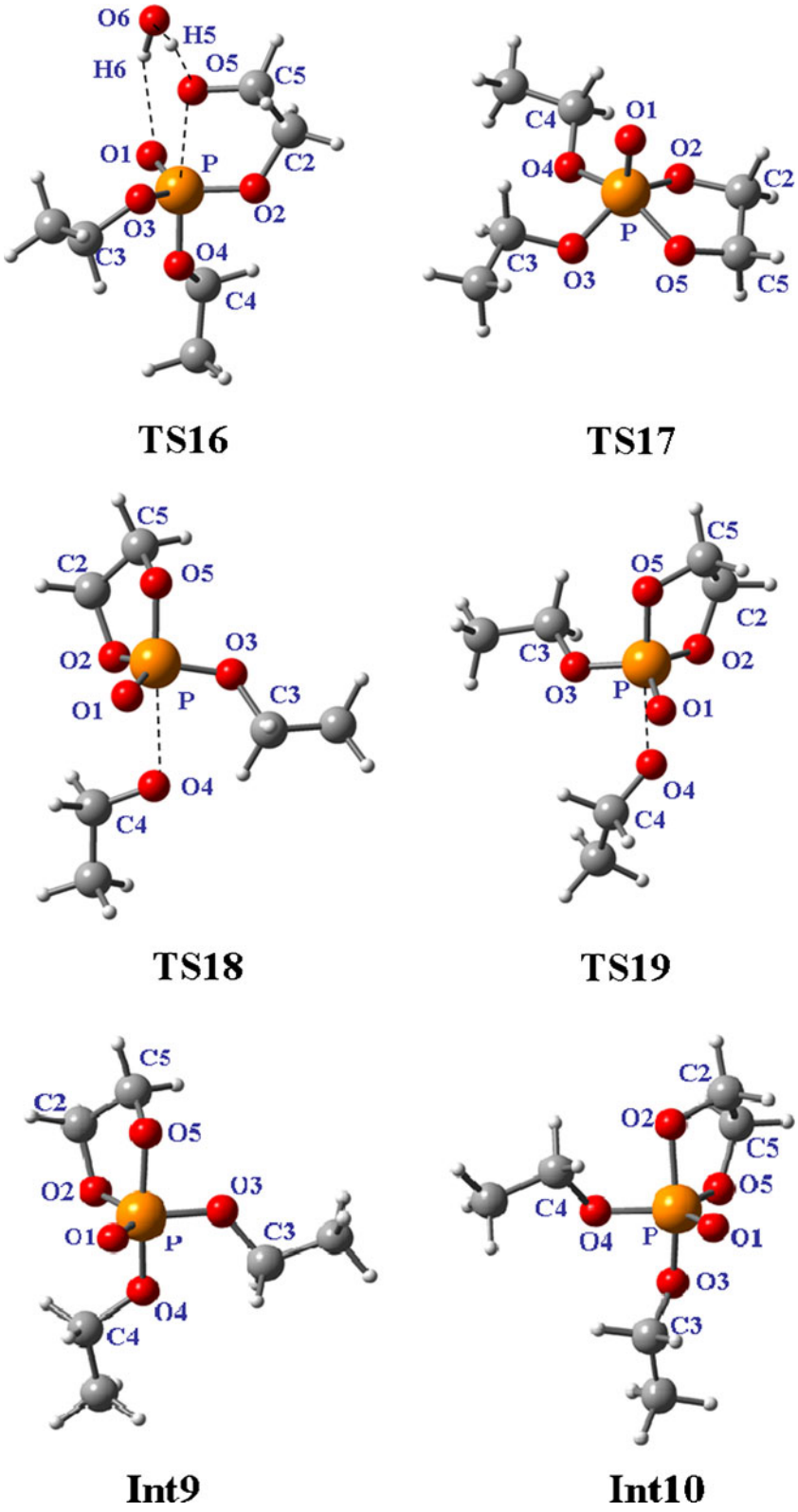

Fig. 8 Solution phase optimized structures of the transition states and the intermediates involved in the alkaline hydrolysis of DEHEP

than those (49.5 and 25.7 kcalmol^{-1}) of the acyclic ones from TEP. The hydrolysis of both TEP and DEHEP can be catalyzed by hydroxide because of the considerable decrease of the formation energy barrier of phosphorane. Especially, the more rapid base-catalyzed hydrolysis of DEHEP than TEP can be

attributed to the extremely lower formation barriers of cyclic phosphoranes than those of acyclic ones.

Acknowledgments This work was supported by the grants from the National Natural Science Foundation of China (No. 20907002), the Beijing Nova Program (No. 2009B08) and the Training Program Foundation for the Beijing Municipal Natural Science Foundation (No. 8113031).

References

1. Gnewuch CT, Sosnovsky G (1997) Chem Rev 97:829–1014
2. Wang PG, Xian M, Tang X, Wu X, Wen Z, Cai T, Janczuk AJ (2002) Chem Rev 102:1091–1134
3. Morimoto K, Tanaka A, Yamaha T (1983) Carcinogenesis 4:1455–1458
4. Singer B, Grunberger D (1983) Molecular biology of mutagens and carcinogens. Plenum, New York
5. Saffhill R (1984) Carcinogenesis 5:621–625
6. Beranek DT (1990) Mutat Res 231:11–30
7. Singer B (1976) Nature 264:333–339
8. Singer B, Spengler S, Bodell WJ (1981) Carcinogenesis 2:1069–1073
9. Swenson DH, Harbach PR, Trzos RJ (1980) Carcinogenesis 1:931–936
10. Singer B (1975) Progress in nucleic acid research and molecular biology. Academic, New York
11. Lown JW, McLaughlin LW (1979) Biochem Pharmacol 28:1631–1638
12. Walles S, Ehrenberg L (1968) Acta Chem Scand 22:2727–2729
13. Gutin PH, Hilton J, Fein VJ, Allan AE, Rottman A, Walker MD (1977) Cancer Res 37:3761–3765
14. Erickson LC, Bradley MO, Kohn KW (1977) Cancer Res 37:3744–3750
15. Hilton J, Bowie DL, Gutin PH, Zito DM, Walker MD (1977) Cancer Res 37:2262–2266
16. Gamper HB, Tung ASC, Straub K, Bartholomew JC, Calvin M (1977) Science 197:671–674
17. Swenson DH, Frei JV, Lawley PD (1979) J Natl Cancer Inst 63:1469–1473
18. Brown DM, Todd AR (1952) J Chem Soc p 44–51
19. Lawley PD, Brookes P (1963) Biochem J 89:127–138
20. Bannon P, Verly WG (1972) Eur J Biochem 31:103–111
21. Shooter KV (1976) Chem Biol Interact 13:151–163
22. Swenson DH, Farmer PB, Lawley PD (1976) Chem Biol Interact 15:91–100
23. Conrad J, Muller N, Eisenbrand G (1986) Chem Biol Interact 60:57–65
24. Zeller WJ, Lijinsky W, Eisenbrand G (1985) J Cancer Res Clin Oncol 109:A46
25. Zeller WJ, Fruhauf S, Chen G, Eisenbrand G, Lijinsky W (1989) Cancer Res 49:3267–3270
26. Lopez X, Dejaegere A, Karplus M (2001) J Am Chem Soc 123:11755–11763
27. Kirby AJ, Lima MF, da Silva D, Nome F (2004) J Am Chem Soc 126:1350–1351
28. Kirby AJ, Dutta-Roy N, da Silva D, Goodman JM, Lima MF, Roussev CD, Nome F (2005) J Am Chem Soc 127:7033–7040
29. Kirby AJ, Lima MF, da Silva D, Roussev CD, Nome F (2006) J Am Chem Soc 128:16944–16952
30. Klahn M, Rosta E, Warshel A (2006) J Am Chem Soc 128:15310–15323
31. Berente I, Beke T, Naray-Szabo G (2007) Theor Chem Acc 118:129–134
32. Rosta E, Kamerlin SCL, Warshel A (2008) Biochemistry 47:3725–3735
33. Yang Y, Yu HB, York D, Elstner M, Cui Q (2008) J Chem Theor Comput 4:2067–2084
34. Kirby AJ, Tondo DW, Medeiros M, Souza BS, Priebe JP, Lima MF, Nome F (2009) J Am Chem Soc 131:2023–2028
35. Kamerlin SCL, Williams NH, Warshel A (2008) J Org Chem 73:6960–6969
36. Florian J, Warshel A (1998) J Phys Chem B 102:719–734
37. Aqvist J, Kolmodin K, Florian J, Warshel A (1999) Chem Biol 6: R71–R80
38. Menegon G, Loos M, Chaimovich H (2002) J Phys Chem A 106:9078–9084
39. Chang NY, Lim C (1997) J Phys Chem A 101:8706–8713
40. Chang NY, Lim C (1998) J Am Chem Soc 120:2156–2167
41. Iche-Tarrat N, Barthelat JC, Rinaldi D, Vigroux A (2005) J Phys Chem B 109:22570–22580
42. Iche-Tarrat N (2010) J Mol Struc THEOCHEM 941:56–60
43. Brown DM, Todd AR (1952) J Chem Soc p 52–58
44. Zhou DM, Taira K (1998) Chem Rev 98:991–1026
45. Lim C, Tole P (1992) J Am Chem Soc 114:7245–7252
46. Lim C, Tole P (1992) J Phys Chem 96:5217–5219
47. Tole P, Lim CM (1993) J Phys Chem 97:6212–6219
48. Tole P, Lim C (1994) J Am Chem Soc 116:3922–3931
49. Liu Y, Gregersen BA, Lopez X, York DM (2005) J Phys Chem B 109:19987–20003
50. Lopez CS, Faza ON, de Lera AR, York DM (2005) Chem Eur J 11:2081–2093
51. Liu Y, Gregersen BA, Hengge A, York DM (2006) Biochemistry 45:10043–10053
52. Lopez X, Dejaegere A, Leclerc F, York DM, Karplus M (2006) J Phys Chem B 110:11525–11539
53. Lopez X, Schaefer M, Dejaegere A, Karplus M (2002) J Am Chem Soc 124:5010–5018
54. Range K, McGrath MJ, Lopez X, York DM (2004) J Am Chem Soc 126:1654–1665
55. Westheimer FH (1968) Acc Chem Res 1:70–78
56. Brown DM, Usher DA (1963) Proc Chem Soc p 309–310
57. Brown DM, Usher DA (1965) J Am Chem Soc p 6547–6558
58. Brown DM (1974) Basic principles in nucleic acid chemistry. Academic, New York
59. Kuimelis RG, McLaughlin LW (1998) Chem Rev 98:1027–1044
60. Tomasi J, Persico M (1994) Chem Rev 94:2027–2094
61. Cossi M, Barone V, Cammi R, Tomasi J (1996) Chem Phys Lett 255:327–335
62. Mineva T, Russo N, Sicilia E (1998) J Comput Chem 19:290–299
63. Becke AD (1993) J Chem Phys 98:5648–5652
64. Lee CT, Yang WT, Parr RG (1988) Phys Rev B 37:785–789
65. Cossi M, Scalmani G, Rega N, Barone V (2002) J Chem Phys 117:43–54
66. Cossi M, Rega N, Scalmani G, Barone V (2003) J Comput Chem 24:669–681
67. Banas P, Jurecka P, Walter NG, Sponer J, Otyepka M (2009) Methods 49:202–216
68. Rios-Font R, Rodriguez-Santiago L, Bertran J, Sodupe M (2007) J Phys Chem B 111:6021–6077
69. Mayaan E, Range K, York DM (2004) J Biol Inorg Chem 9:807–817
70. Liu Y, Lopez X, York DM (2005) Chem Commun 31:3909–3911
71. Tidor B, Karplus M (1994) J Mol Biol 238:405–414
72. Frisch MJ, Trucks GW, Schlegel HB, Scuseria GE, Robb MA, Cheeseman JR, Scalmani G, Barone V, Mennucci B, Petersson GA, Nakatsuji H, Caricato M, Li X, Hratchian HP, Izmaylov AF, Bloino J, Zheng G, Sonnenberg JL, Hada M, Ehara M, Toyota K,

Fukuda R, Hasegawa J, Ishida M, Nakajima T, Honda Y, Kitao O, Nakai H, Vreven T, Montgomery JA Jr, Peralta JE, Ogliaro F, Bearpark M, Heyd JJ, Brothers E, Kudin KN, Staroverov VN, Kobayashi R, Normand J, Raghavachari K, Rendell A, Burant JC, Iyengar SS, Tomasi J, Cossi M, Rega N, Millam NJ, Klene M, Knox JE, Cross JB, Bakken V, Adamo C, Jaramillo J, Gomperts R, Stratmann RE, Yazyev O, Austin AJ, Cammi R, Pomelli C, Ochterski JW, Martin RL, Morokuma K, Zakrzewski VG, Voth GA, Salvador P, Dannenberg JJ, Dapprich S, Daniels AD, Farkas Ö, Foresman JB, Ortiz JV, Cioslowski J, Fox DJ (2009) Gaussion 09, Revision B.01. Gaussian Inc, Wallingford

73. Aksnes G, Bergesen K (1966) Acta Chem Scand 20:2508–2514
74. Thatcher GRJ, Kluger R (1989) Adv Phys Org Chem 25:99–265
75. Kluger R, Covitz F, Dennis E, Williams LD, Westheimer FH (1969) J Am Chem Soc 91:6066–6072
76. Kluger R, Taylor SD (1990) J Am Chem Soc 112:6669–6671
77. Kluger R, Taylor SD (1991) J Am Chem Soc 113:5714–5719
78. Shiiba T, Komiyama M (1992) Tetrahedron Lett 33:5571–5574
79. Kuimelis RG, McLaughlin LW (1995) Nucleic Acids Res 23:4753–4760
80. Kuimelis RG, McLaughlin LW (1995) J Am Chem Soc 117:11019–11020
81. Kuimelis RG, McLaughlin LW (1996) Biochemistry 35:5308–5317
82. Thomson JB, Patel BK, Jimenez V, Eckart K, Eckstein F (1996) J Org Chem 61:6273–6281
83. Kuimelis RG, McLaughlin LW (1997) Bioorgan Med Chem 5:1051–1061